Contents lists available at ScienceDirect

Nuclear Inst. and Methods in Physics Research, A

journal homepage: www.elsevier.com/locate/nima

Improvement of the performance of a cryo-cooled monochromator at SSRF. Part II: Angular stability of the exit beam

Wu Jiaxing [a,b], Gong Xuepeng [c], Song Yuan [c], Chen Jiahua [a,b], Zhu Wanqian [a,b], Liu Yun [a,b], Fan Yichen [a,b,d,*], Jin Limin [a,b,*]

[a] *Shanghai Institute of Applied Physics, Chinese Academy of Sciences, Shanghai 201204, China*
[b] *Shanghai Advanced Research Institute, Chinese Academy of Sciences, Shanghai 201210, China*
[c] *Changchun Institute of Optics, Fine Mechanics and Physics, Chinese Academy of Sciences, Changchun 130033, China*
[d] *University of Chinese Academy of Sciences, Beijing 100049, China*

A B S T R A C T

The angular stability of the crystals used in the monochromator is crucial for the beam position, the flux and the resolution for the synchrotron based hard X-ray beamline. In this paper, we report a performance optimization to a double-crystal monochromator (DCM) which has served for nearly 10 years at Shanghai Synchrotron Radiation Facility (SSRF). By upgrading the design of the clamping and the cooling to the 2nd crystal, the layout of the LN_2 circuit, the structure of the 2nd crystal assembly and the thermal insulation as well as the temperature stabilization system, the resulted angular stability of the crystals in working condition (LN_2 circulation) tested by the angular stability of the exit beam has been greatly improved from approximately 500 nrad RMS/2 h up to better than 200 nrad RMS/2 h in vertical direction (pitch rotation of the crystals) and better than 300 nrad RMS/2 h in horizontal direction (roll rotation of the crystals) respectively, which meets the requirement by 300 nrad RMS/2 h in user experiments of the BSL-2 macromolecular crystallography beamline (P2, BL10U2).

1. Introduction

After decades of vigorous development and continuous progress of the related technologies, synchrotron radiation has played increasingly important role in various disciplines and has been globally used by researchers [1–3]. Shanghai Synchrotron Radiation Facility (SSRF) which started operation in 2009 is a typical 3rd-generation synchrotron light source in mainland China. It has been extensively supported the scientific research and the industry R&D, and its contribution to scientific and technological progress has been highlighted with the various emerging scientific achievements [4].

The BSL-2 macromolecular crystallography beamline (P2, BL10U2), one of the phase II beamlines being built in SSRF, is devoted to study the structure of virus particles using X-ray crystal diffraction. This beamline is equipped with an undulator as the source and a cryo-cooled double crystal monochromator (DCM) to select the narrow band of wavelengths of beam needed from the continuous X-ray spectrum and to focus the beam at the sample position [5–10].

The focused spot at the sample of the P2 experimental station is only $20 \times 10~\mu m^2$ (H × V). It is expected that the experiments can be completed efficiently without adjusting and optimizing the beam during the selecting of X-ray energy. Therefore, the angular stability

of the exit beam are demanding, and whose quality will directly affect the stability of the luminous flux and spot position at the sample. The angular stability of the exit beam is usually converted into the amount of variation in the horizontal and vertical angular displacements, which correspond to those in roll and pitch directions of the 1st and 2nd crystals respectively. It should be noted that the angular stability of the crystals in pitch direction is much more crucial. It affects the position of the exit beam, and has a direct effect on the output flux of the monochromator. For a cryo-cooled DCM, the most direct influencing factor to the angular stability of the exit beam is the vibration to the crystals induced by LN_2 circulation, which is mainly derived from the turbulent state of LN_2 in the loop [11–13]. Therefore, the cooling efficiency of the 1st crystal and the vibration absorption of circulating LN_2 should be taken into account. In addition, the sufficient attention on the improvement of structural rigidity and thermal stability should also be given. Excellent structural rigidity and thermal stability can make the crystals resist the vibration caused by circulating LN_2, and keep the related structural parts away from the cold shrinkage and thermal expansion caused by low temperature and high thermal load scattering as much as possible. All these factors will certainly affect the long-term angular stability.
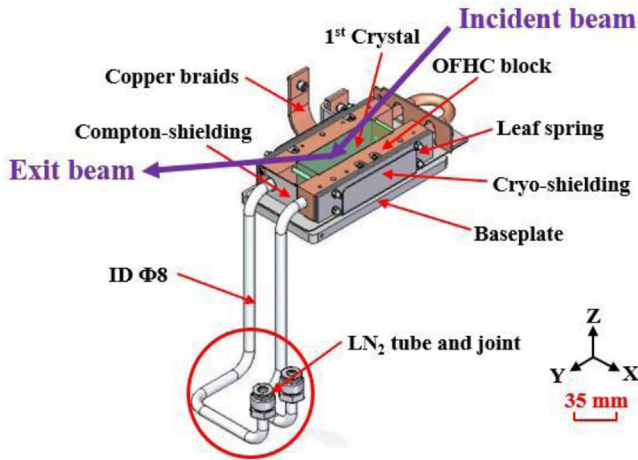

Fig. 1. Clamping and cooling method of the 1st crystal.

Table 1
The related working parameters of the 1st crystal.

Type of the light source	Undulator
Overall power of the undulator (kW)	2.6
Distance between the rotation center of the 1st crystal to the light source (m)	24.5
Acceptance angle to the incident beam (μrad^2) (H $\times$ V)	100 $\times$ 50
Theoretical thermal load (W)	140.54
Working energy range (keV)	5–18
Projected area of beam spot @ 5 keV (mm^2)	2.6 $\times$ 4.6
Single-sided clamping stress (MPa)	0.45
Energy resolution $\Delta E/E$ (@12.7 keV)	$<2 \times 10^{-4}$
Comprehensive slope error in meridian direction (μrad RMS)	<1.5

In this paper, the optimization design is performed to meet the experimental requirements of the P2 beamline based on a cryo-cooled DCM (Bruker Corporation, Karlsruhe, Germany) which has served for nearly 10 years at SSRF. The original cooling method of the 1st crystal is verified to satisfy the actual working conditions with finite element analysis (FEA). Emphasis will be given to upgrade the internal related structures to optimize the angular stability of the exit beam. The relative angular stability of the crystals within 2 h is tested under LN$_2$ circulation state at key energy positions of P2 beamline. Testing accessorial tools and laser interferometer components are implemented, and thus the angular stability of the exit beam could be investigated and characterized.

2. Experimental

2.1. Cooling effect simulation for the old design of the 1st crystal's clamping and cooling

Before any structural optimization started, an evaluation for the old clamping and cooling design for the 1st crystal shall be done as the base line of our work. The 1st crystal adopts the side clamping and indirect cryo-cooling method as shown in Fig. 1. The relevant working parameters are listed in Table 1.

The cooling effect of the 1st crystal with the original clamping and cooling method was thermally analyzed via FEA. The parameters of LN$_2$ are listed in Table 2. As for convection cooling, the key factor to improve the cooling effect is to increase the convection heat transfer coefficient (film coefficient, h, W/(m^2 K)) at the cooling interface. This coefficient is often used to evaluate the cooling capacity. It is calculated by the following formulas:
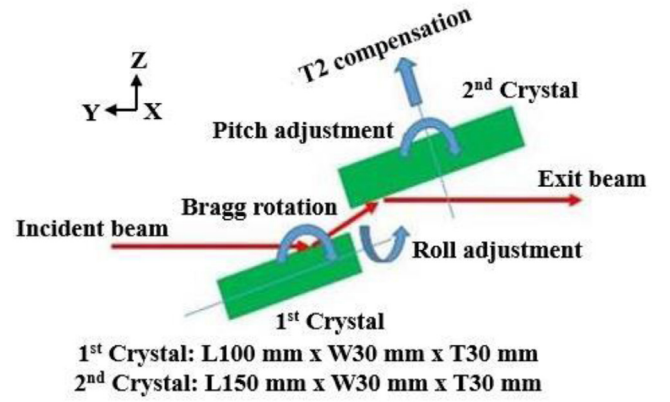
$$h = \frac{N_u k}{D} \tag{1}$$

Fig. 2. Definition for the motion axis of the crystals.

where h (W/(m^2 K)) is the convection heat transfer coefficient, N_u is the Nusselt number, k (W/(m K)) is the thermal conductivity of the cooling medium, and D (mm) is the diameter of the circular cooling tube.

According to Dittus–Boelter formula:

$$N_u = 0.023 R_e^{0.8} P_r^{0.4} \tag{2}$$

$$R_e = \frac{\rho v D}{\mu} \tag{3}$$

$$P_r = \frac{\mu C_p}{k} \tag{4}$$

That is:
$$h = \frac{0.023(\rho v)^{0.8} C_p^{0.4} k^{0.6}}{\mu^{0.4} D^{0.2}} \tag{5}$$

where Re is the Reynolds number, which reflects the influence of convection intensity on heat transfer, Pr is the Prandtl number, which reflects the influence of fluid properties, ρ (kg/m^3), v (m/s), μ (uPa s) and C_p (J/(g K)) are the density, flow velocity, viscosity, and specific heat of the cooling medium, respectively.

2.2. The improvement of the clamping and cooling method of the 2nd crystal

The motion axis for the crystals is defined as shown in Fig. 2. The rotation center of Bragg axis is located in the 1st crystal's surface with the distance of 30 mm away from the downstream end face, perpendicular to the incident beam. The alignment for crystals can be achieved by tuning the angle roll of the 1st crystal and the angle pitch & translation along surface normal of the 2nd crystal to meet the focus condition, that the gap between the incident and the exit beam shall be 25 mm constant.

The old design for clamping and cooling the 2nd crystal is shown in Fig. 3(a). A bottom clamping and indirect LN$_2$ back flow cooling way is adopted, which has two main drawbacks

Firstly, the LN$_2$ flowing transmits vibration to the 2nd crystal when it passing through the base plate, thus affect the stability for pitch rotation.

Secondly, it is much easier to cause slope error in meridian direction (Y direction in Fig. 3(a)) for the direct cooling than indirect one due to micro-level mismatch between bottom surface of the 2nd crystal and its base plate caused by non-uniform screws tightening. As a result, the energy resolution of the monochromator reduces for defocus and coma generated.

Here we consider a new design using a side clamping and a more indirect cooling strategy. The reason is that it is not only greatly improving above situations due to less vibration and slope error caused to the crystals, but additionally ensures their resolving power due to better phase matching for more uniform lattice expansion between the

Table 2

The related parameters of LN$_2$.

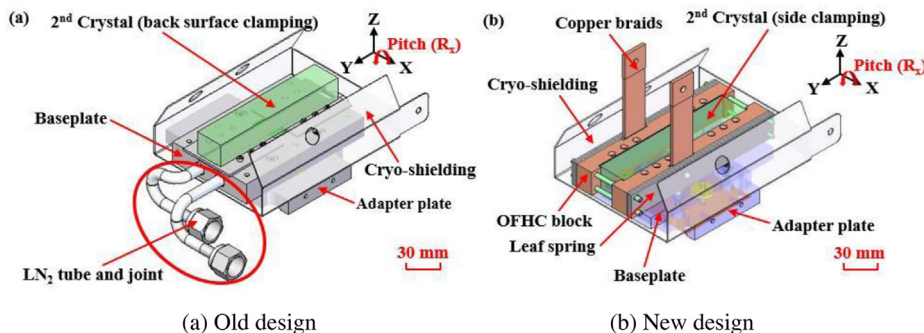| Density (ρ, kg/m^3)	Specific heat (C_p, J/(g K))	Viscosity (μ, uPa s)	Thermal conductivity (k, W/(m K))	Circuit flow (q, L/min)	Film coefficient (h, W/(m^2 K))	Initial temperature (T, K)
795.52	2.0482	146.5	0.14086	3.2	3000	77

Fig. 3. The clamping and cooling design for the 2nd crystal (a) old design and (b) new design introduced in this work.
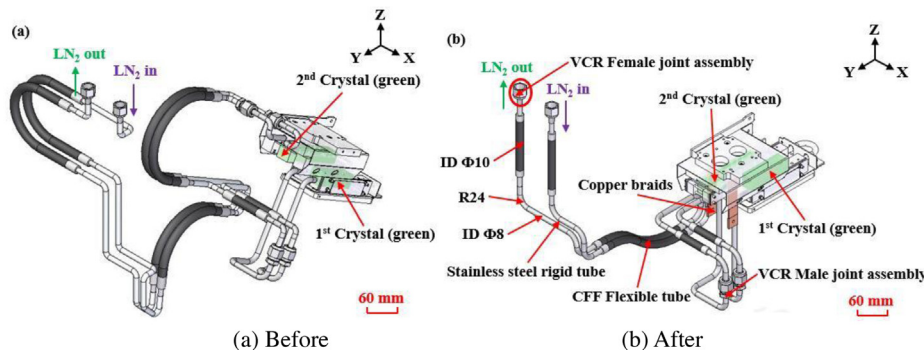

Fig. 4. Layout of LN$_2$ circuit before (a) and after (b) the improvement.

2nd and 1st crystal as resulted to a smaller heat load (less than 1 Watt) on the 2nd crystal.

The re-designed clamping and cooling mechanism for the 2nd crystal is shown in Fig. 3(b). A pieces of indium foil (0.5 mm thick) is used between the crystal and the OFHC block on each sides to increase thermal conductivity. Three pieces of spring steel reed with four M4 Titanium bolts are mounted to ensure a good contact between the crystal and the OFHC block. A pair of copper braids (10 cm in length), which connect to the LN$_2$ tubes of the 1st crystal assembly, are attached to the OFHC blocks for cooling power transferring. In order to avoid back side touching by the base plate that may generate surface error like in the back clamping way, the crystal has been cut by 6 mm in thick, which substantially improves the uniformity compared with the old design.

2.3. The improvement of the layout of the LN$_2$ circuit inside the chamber

The main goal of improving the LN$_2$ circuit inside the chamber is to have less turns thus less LN$_2$ turbulence produced in the loop. The layout of LN$_2$ circuit inside the monochromator is shown in Fig. 4(a). Both crystals are indirectly cooled by LN$_2$ that going through the attached copper blocks of the 1st crystal and the base plate of the 2nd crystal in turn. At the same time the LN$_2$ flow introduces vibration to the circuit loops that worsen the stability for pitch and roll specifications, which cause flux and resolution loss for beam reaching to the sample. The improved structure of the LN$_2$ circuit is shown in Fig. 4(b). The 1st crystal's cooling remains the indirect way, while that for the 2nd crystal is modified to a more indirect way using a pair of copper braids with length of 10 cm that connected to the LN$_2$ tubes of the 1st

crystal assembly. The new circuit is mainly composed of three parts: flexible hose, rigid tube and VCR female connector assembly. They are sealed and connected by TIG welding. Each of the flexible hose is help to compensate the displacement required for each motion axis of the crystals, meanwhile effectively reduce the vibration generated by the circulating LN$_2$ flow. We select the series type of ORVB-10CFF flexible hoses made by Osaka Rasenkan Kogyo Co., Ltd, with the inner diameter and lining of 10 mm. The flexible hoses are made of special thermal insulation and vibration reduction materials. An example is shown in Fig. 5. The rigid tube with inner diameter of 8 mm is made of stainless steel (1Cr18Ni9Ti, where the content of carbon, chromium, and nickel are 1‰, 18‰, and 9‰, respectively). The design of the bending radius (R24 mm) of the rigid tube has taken the processing capacity of the existing universal pipe bender into account. The 1/2 inch VCR female joint assembly, at both ends of the circuit, has been applied to seal the LN$_2$ pipe socket component mounted on the feedthrough flange of the chamber. The improved LN$_2$ circuit shall sufficiently suppress the vibration of the circulating LN$_2$ and take the cooling effect of the crystals into account, thus that the flux and angular rotation stability are effectively improved.

2.4. The structural improvement of the 2nd crystal assembly

As mentioned in Section 1, as the crystals' pitch rotation stability is much more crucial for downstream beam's quality, the improvement work is mainly focused on the 2nd crystal assembly since the fine-tune mechanism in pitch direction is mounted on this part.

After comprehensively considering the structural characteristics and working conditions of the monochromator, the factors affecting the stability in pitch rotation can be divided into three parts

Fig. 5. Flexible hose of series ORVB-10CFF (Osaka Rasenkan Kogyo Co,. Ltd)
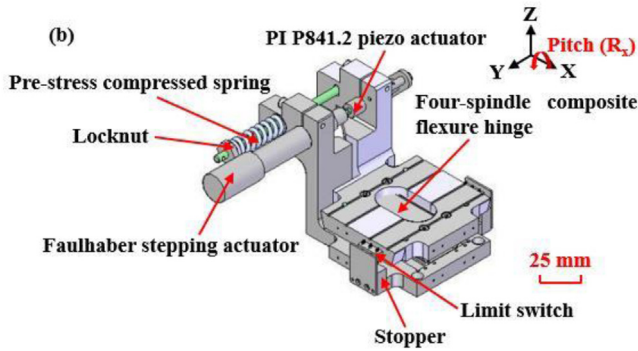

Fig. 6. The angular fine-tune mechanism of the 2nd crystal.

(1) The vibration caused by circulating LN_2 flow;

(2) The variation of the posture of the 2nd crystal in pitch rotation caused by the elastic deformation of the flexure hinges;

(3) The surrounding low frequency (1~50 Hz) vibration due to the low natural frequency of the crystal assembly.

In conclusion, we mainly proceed the upgrade from the corresponding three aspects:

(1) Improve the clamping and indirect cooling method of the 2nd crystal (Section 2.2);

(2) Increase the angular stiffness of the flexure hinge;

(3) Reduce the weight of the relevant structural parts.

The angular fine-tuning of the 2nd crystal adopts a tangent bar mechanism, as shown in Fig. 6. The linear displacement (δL) of the input end and the angular displacement (θ) of the output end are in accordance with a tangent relationship. L is the span between the axis of the displacement input end and the rotation center of the mechanism. Driven by a linear stepper motor and a piezo ceramic actuator pre-tightened to each other, the crystal rotates around the axis of the rotation center of the flexure hinge to achieve fine-tuning in pitch
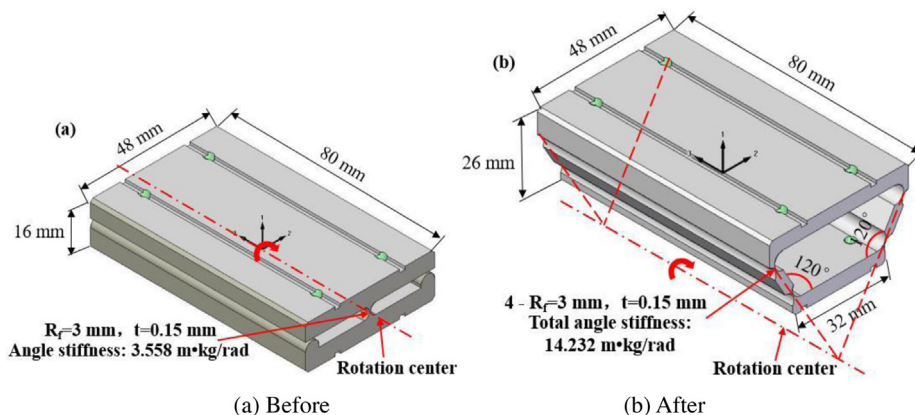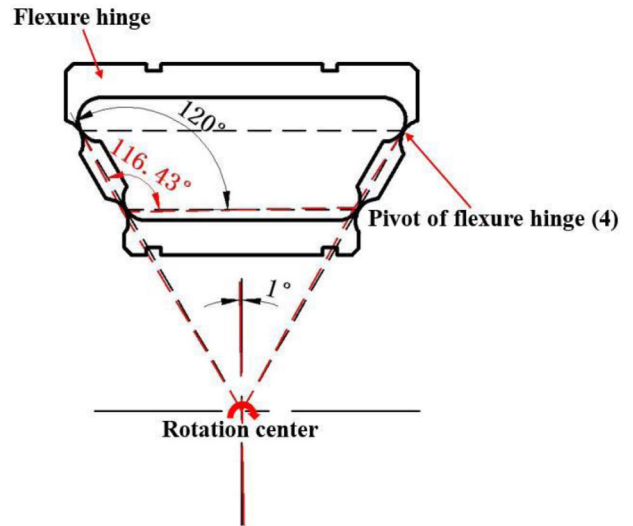

Fig. 8. Angular displacement of a single hinge of the four-axis composite flexure hinge.

direction of the 2nd crystal.

$$\Delta L = L \cdot \tan \theta \tag{6}$$

The improvement shall focus on optimizing the angular stiffness of the weakest part in the assembly i.e., the flexure hinge. The previous design applies a single-axis flexure hinge made of beryllium bronze material (QBe1.9, yield strength $\sigma_s = 1.03$ GPa, elastic modulus $E_f = 130$ GPa) as the rotation axis, as shown in Fig. 7(a). The flexure hinge is based on the linear and angular displacement generated by the elastic deformation of the material. It overcomes the mechanical friction and backlash caused by the conventional mechanical motion, and has been applied to the micron-level adjustment unit in precision mechanism. The improved flexure hinge adopts an isosceles trapezoidal four-axis composite structure as shown in Fig. 7(b). The obtuse angle of this isosceles trapezoid is 120°. The angular stiffness of the flexible hinge with the new structure is 14.232 m kg/rad [14], which is four times as much as that of the former design. Each hinge of this structure is under the premise of no plastic deformation, and its maximum allowable angular displacement is:

$$\varphi_{\max} = \frac{3\pi\sigma s}{4Ef} \sqrt{\frac{R_f}{t}} = 4.78° \tag{7}$$

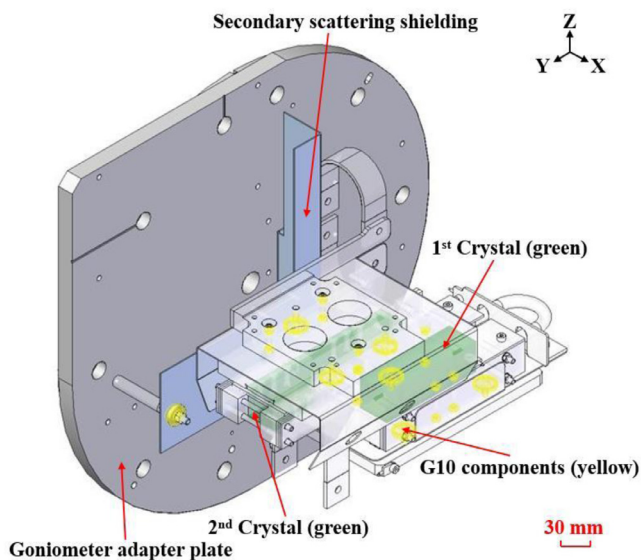where R_f is the rotation radius of the structure and t is the minimum thickness at the hinge.

(a) Before   (b) After

Fig. 7. Structure of the flexure hinge (a) before and (b) after the improvement.

Fig. 9. Mounting locations of G10 components.

Fig. 11. Full assembly of the internal mechanism of the monochromator after the improvement.

The 2nd crystal should acquire motion range of ±1° in pitch direction. The improved flexure hinge can be simplified into a planar four-link mechanism. The mechanism inversion method is applied to calculate the angular displacement of a single hinge, as shown in Fig. 8. It can be seen that, when the entire hinge mechanism rotates around its rotation center for 1°, the angular displacement of a single hinge would be $\varphi = 3.56° < \varphi_{max} = 4.78°$. Therefore, the improved design of flexure hinge can well satisfy the required motion range with each single hinge intact and free of plastic deformation.

2.5. The improvement of the thermal insulation and temperature stabilization system

During online operation, when the inside of the monochromator chamber is in ultra-high vacuum (with a base pressure better than 10^{-7} Pa), the internal structure will shrink and expand with LN2 circulation and high thermal load scattering. These effect will worsen the long-term (≥2 h) stability for the crystals motions. Therefore, good thermal insulation and temperature stabilization has to be taken into consider. In the original concept for thermal isolation, the low thermal conductivity ceramic is used between different parts, while for temperature stabilization, an OFHC block is used on the goniometer's adaptor plate,
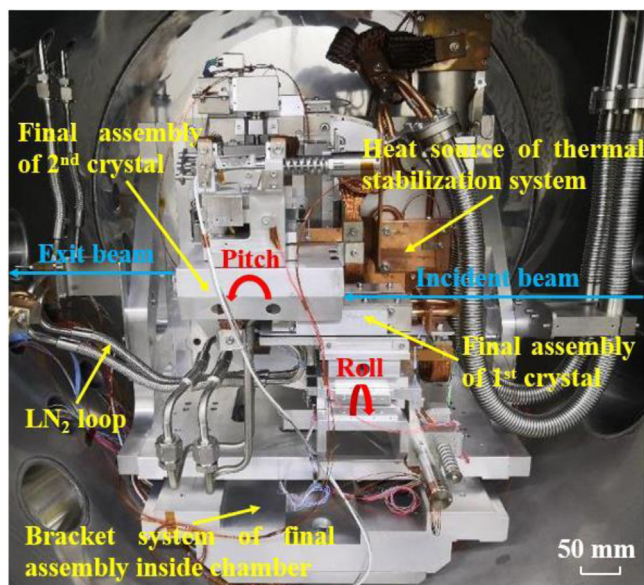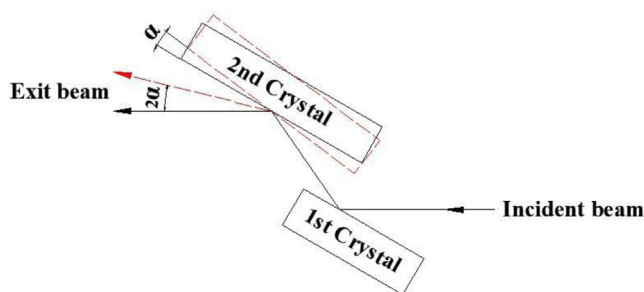

Fig. 12. The relationship between angular variation of the crystals and exit beam in pitch direction.

which is circulated with deionized water of constant temperature (25 °C) and connected with several copper braids to different parts. After long period of operation, it is found that the thermal insulation effect of such ceramic material is not good especially when the ambient temperature goes below 0 °C. And the low-frequency vibration (10–50 Hz) produced by circulating deionized water also have a bad effect to the

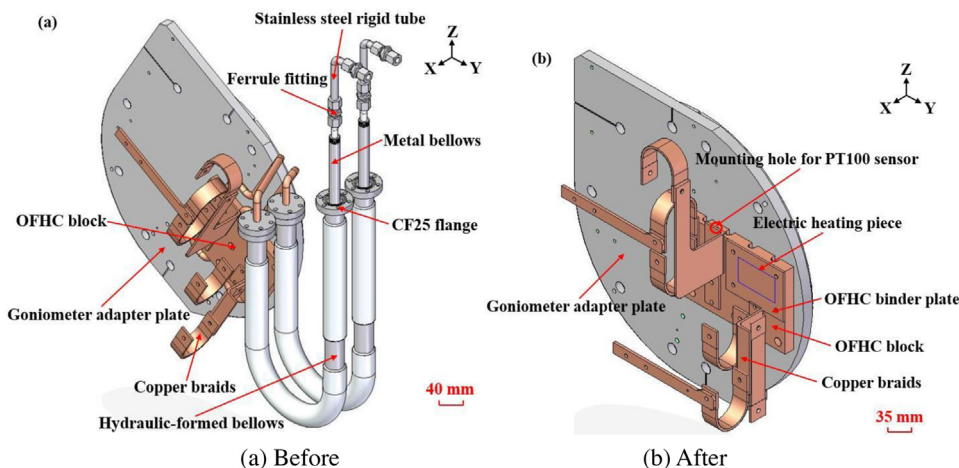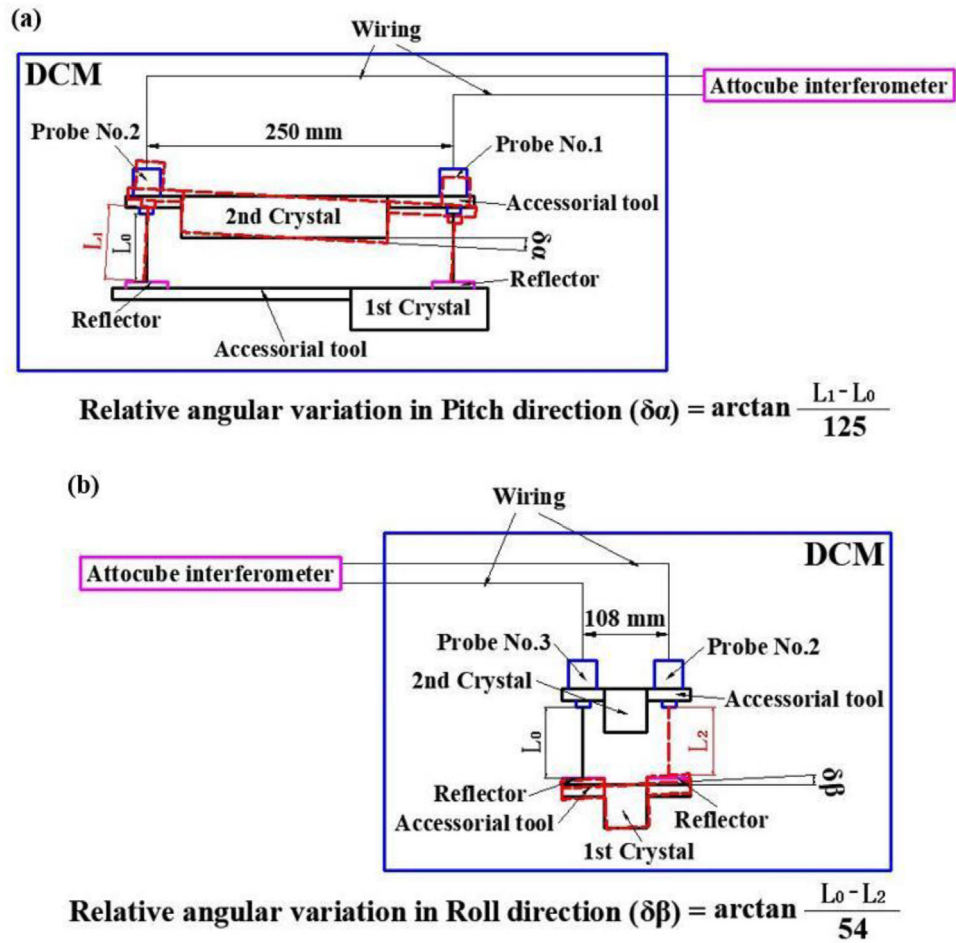**Fig. 10.** The temperature stabilization system (a) old and (b) updated.

$$\text{Relative angular variation in Pitch direction } (\delta\alpha) = \arctan\frac{L_1 - L_0}{125}$$

$$\text{Relative angular variation in Roll direction } (\delta\beta) = \arctan\frac{L_0 - L_2}{54}$$

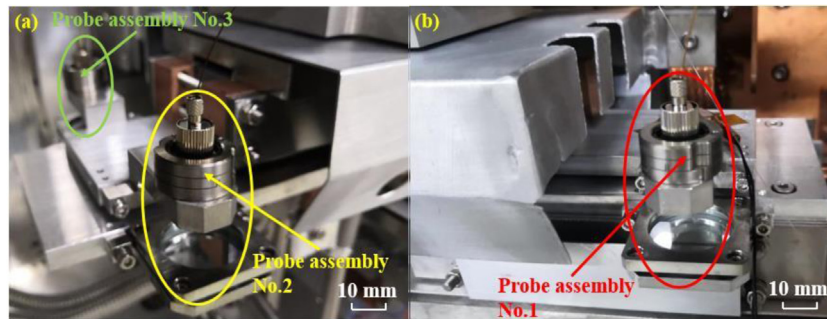**Fig. 13.** The measuring principle for evaluating the pitch (a) and roll (b) variation of the crystals.

Fig. 14. (a) Full assembly of probe components No.2, No.3 and (b) No.1 for the measurement of relative angular stability of the crystals under LN_2 circulation.

long-term stability of crystal. Therefore, it is necessary to improve the thermal insulation and temperature stabilization system based on the original structure.

The material polyimide (G10) is believed to be able to solve above problem due to its pretty low thermal conductivity (0.2076 W/m·K) in the low temperature range (−190~0 °C) better than ceramic. We designed and fabricated the same thermal isolation structures with G10 and mounted on the same positions replacing the original ceramic. The finished structure is as shown in Fig. 9.

For temperature controlling for the new system, we use the model 336 temperature controller (Lake Shore Cryotronics, Inc., USA). A PT100 platinum resistance is connected to the input terminal, while a model HK5399R9.1L60A electric heater (Minco & Co., Ltd. USA) is connected to the output terminal. Such system configuration is supposed to keep the temperature variation of the controlled object within ±0.3 °C.

The PT100 platinum resistance is inserted into the mounting hole on the OFHC block, while the electric heater is pressed to mounting on the OFHC block by a copper plate. During real operation, the target temperature of the PT100 platinum resistance is set to 25 °C in the temperature controller. And the electric heater will be heated with a power of 25 W. As a result, the OFHC block would be the heat source of the internal temperature stabilization system of the monochromator, with the temperature stability of 25 ± 0.3 °C. Several copper braids are used to connect the heat source to different structural parts for heat conduction. The improved temperature stabilization system has effectively avoided the low frequency vibration induced by circulating deionized water.

The design for the original and updated temperature stabilization systems is shown in Fig. 10.

The full assembly of the internal mechanism of the monochromator after the improvement is shown in Fig. 11.

2.6. Measurement of relative stability under LN_2 circulation

The angular stability performance for the design updated monochromator can be indirectly investigated by measuring the pitch and roll variation of the crystals with LN_2 circulation. The cryo-cooler (Accel Corporation, Germany) has been applied for this measurement. The closed loop of LN_2 consists of a pair of flexible braided pipes which separately connected to the cryo-cooler, the LN_2 pipe socket components on the monochromator and the LN_2 circuit inside. In working condition, the crystal set reflects the incident beam twice thus the angular variation for the exit beam is twice as much as the pitch variation of the crystals, as shown in Fig. 12.

A diagrammatic sketch for the measuring principle of the angular variation of the crystals is shown in Fig. 13. The type of IDS3010 interferometer (Attocube, Germany) is used for tracking beam path variation. Three M15.5/C1.6/FLEX/LT probes (sampling frequency 60 Hz) and diameter reflectors with 30 mm are mounted on the crystals. Probes No. 1 and 2 are mounted along the beam (with a distance of 250 mm), measuring the distance variation in pitch direction for crystals; while probes No. 2 and 3 are mounted perpendicular to the beam (with a distance of 108 mm) checking that in roll direction for crystals. By programming the corresponding algorithm, the data collected by each probe within two hours are converted into the relative angular displacement variation (RMS) in pitch and roll. Full assembly of the measurement module of the relative angular stability of the crystals are shown in Fig. 14.

3. Results and discussions

3.1. Relevant basis for parameter setting of LN_2 circulation

During online operation of the monochromator, the entire cryo-cooler system has to provide enough cooling power for the 1st crystal to minimize the thermally induced meridian slope error. The LN_2 shall be circulated in a laminar flow state in the entire closed loop. There shall be no boiling of circulating LN_2 after dissipating the high heat load on the 1st crystal.

In order to know the cooling performance baseline, a thermal analysis via FEA is done for the 1st crystal, which is shown in Fig. 15. It is shown that the maximum surface temperature on the crystal is 104.54 K, the maximum equivalent stress is 0.16 MPa and the meridian slope error caused by clamping and thermal distortion is 1.23 μrad (RMS). It has been tested that, by setting the LN_2 flow rate at 3.2 L/min, the meridian slope error of the 1st crystal can still meet the operation requirement of 1.5 μrad in the maximum beam power density condition (10.8 W/mm^2, @5 keV). This demonstrates that the original clamping and cooling design of the 1st crystal is effective thus not need to update.

3.2. The angular stability of the exit beam

According to user experiment's requirement, the important working energy points for the monochromator is 16 keV, 12.7 keV, 9 keV, and 5 keV. So we set the test at these energy points to measure the pitch and roll variation. After 10 h when LN_2 circulation turning on when the monochromator thermal stabilized, the data was acquired for the distance variation between the probes and the reflectors. It shows that the angular variation is better than 100 nrad RMS/2 h for pitch and better than 300 nrad RMS/2 h for roll. All of the test results have well satisfied the requirements (better than 300 nrad RMS/2 h). The result for different energy point is shown in Fig. 16.
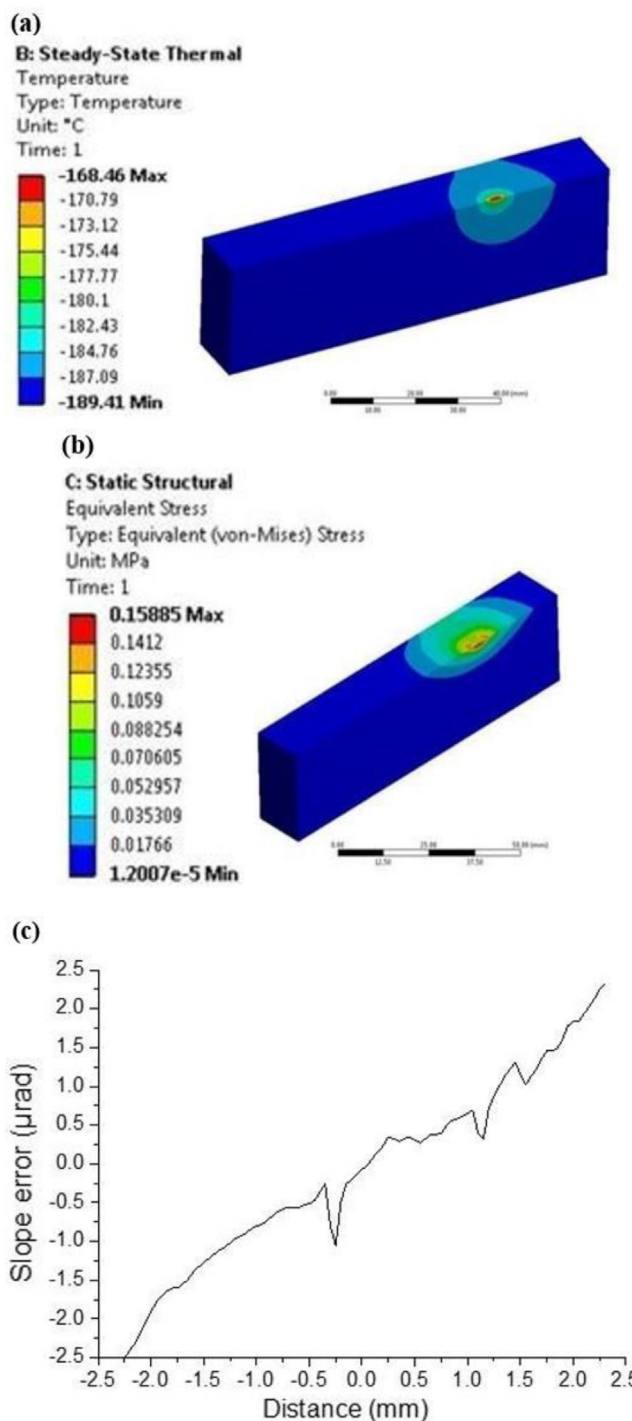
The test results are relisted in Table 3.

Fig. 15. (a) The temperature distribution l, (b) equivalent stress on and (c) curve of slope error in meridian direction of the 1st crystal.

4. Conclusions

To meet the required angular stability (better than 300 nrad RMS/2 h) for the monochromator on the P2 beamline at SSRF, the optimization design of a cryo-cooled monochromator was performed. After a comprehensive analysis for the influencing factors and the structural characteristics, it is found that the original clamping and cooling design of the 1st crystal could satisfy the requirements with proper circulation parameters. In particular, the monochromator has been optimized via the following four aspects:
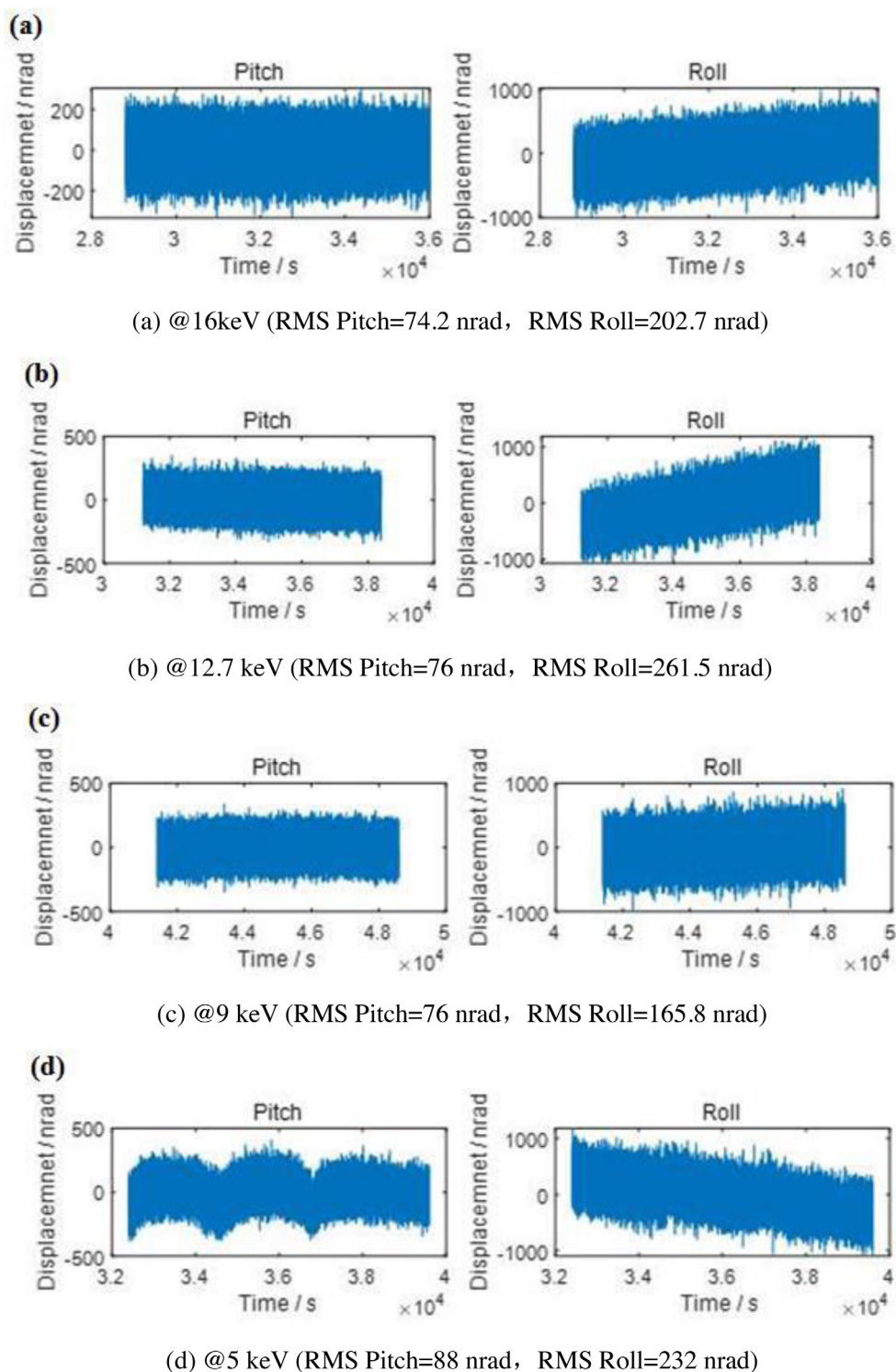
(a) @16keV (RMS Pitch=74.2 nrad，RMS Roll=202.7 nrad)

(b) @12.7 keV (RMS Pitch=76 nrad，RMS Roll=261.5 nrad)

(c) @9 keV (RMS Pitch=76 nrad，RMS Roll=165.8 nrad)

(d) @5 keV (RMS Pitch=88 nrad，RMS Roll=232 nrad)

Fig. 16. The result of the relative angular stability @ (a) 16 KeV, (b) 12.7 keV, (c) 9 keV and (d) 5 keV.

Table 3
The test results of the angular stability of the exit beam.

Pump frequency (Hz)	Flow rate (L/min)	Energy position (keV)	Pitch (nrad RMS/2 h)	Roll (nrad RMS/2 h)
22	3.2	16	**148.4**	**202.7**
		12.7	**152**	**261.5**
		9	**152**	**165.8**
		5	**176**	**232**

(1) To update the clamping and cooling design for the 2nd crystal with the side clamping and indirect contact-type cryo-cooled approaches for the better meridional slope error and vibration isolation;

(2) To optimize the layout of the LN$_2$ circuit for the better turbulence isolation;

(3) To re-design the structure of the 2nd crystal assembly for the better angular stiffness and the higher inherent frequency;

(4) To improve the thermal insulation and temperature stabilization system for the better thermal stability.

With the accessorial tools and interferometer components, the angular stability of the crystals with LN$_2$ circulation at the important working energy point has been tested. The obtained result shows that the angular stability has well greatly improved, which satisfies the design requirement of experiment (better than 300 nrad RMS/2 h). The tested angular stability for pitch is better than 200 nrad RMS/2 h, and that for roll direction is better than 300 nrad RMS/2 h. Specifically, the tested vibration for pitch rotation is 148.4 nrad RMS /2 h @16 keV and that for roll is 165.8 nrad RMS/2 h @9 keV.

CRediT authorship contribution statement

Wu Jiaxing: DCM design and optimization, Writing - original draft. **Gong Xuepeng:** DCM design, Writing - review & editing. **Song Yuan:** DCM motion control and wiring. **Chen Jiahua:** DCM design. **Zhu Wanqian:** DCM design. **Liu Yun:** Cryo-cooler preparation and LN$_2$ circulation. **Fan Yichen:** Methodology, Data acquisition, Analysis, Writing - review & editing. **Jin Limin:** Writing - review & editing.

Declaration of competing interest

The authors declare that they have no known competing financial interests or personal relationships that could have appeared to influence the work reported in this paper.

Acknowledgments

References

[1] C. Kunz, Synchrotron radiation: third generation sources, J. Phys.: Condens. Matter 13 (34) (2001) 7499–7510.

[2] T.A. Ezquerra, M.C. Garcia-Gutierrez, A. Nogales, et al., Introduction to the special issue on applications of synchrotron radiation in polymers science, Eur. Polym. J. 81 (2016) 413–414.

[3] P.S. Rahimabadi, M. Khodaei, K.R. Koswattage, Review on applications of synchrotron-based X-ray techniques in materials characterization, X-Ray Spectrum. 49 (3) (2020) 348–373.

[4] J.H. He, Z.T. Zhao, Shanghai synchrotron radiation facility, Natl. Sci. Rev. 1 (2) (2014) 171–172.

[5] M. Yabashi, H. Yamazaki, K. Tamasaku, et al., Spring-8 standard x-ray monochromators, Proc. SPIE 3773 (1999) 2–13.

[6] T. Mochizuki, Y. Kohmura, A. Awaji, et al., Cryogenic cooling monochromators for the SPring-8 undulator beamlines, Nucl. Instrum. Methods A 467–468 (2001) 647–649.

[7] P. Carpentier, M. Rossat, P. Charrault, et al., Synchrotron monochromator heating problem, cryogenic cooling solution, Nucl. Instrum. Methods A 456 (3) (2001) 163–176.

[8] A.I. Chumakov, I. Sergeev, J.P. Celse, et al., Performance of a silicon monochromator under high heat load, J. Synchrotron Radiat. 21 (2014) 315–324.

[9] C.Y. Xu, W.C. Zhao, G.Q. Pan, et al., Nucl. Instrum. Methods A410 (1998) 293–296.

[10] M.S. Del Rio, Mathon O. Proc. of SPIE 5536 (2004) 157–164.

[11] H. Yamazaki, Y. Matsuzaki, Y. Shimizu, et al., Challenges toward 50 nrad-stability of x-rays for a next generation light source by refinements of SPring-8 standard monochromator with cryo-cooled Si crystals, AIP Conf. Proc. 2054 (2019) 060018–1–060018–5.

[12] H. Yamazaki, H. Ohashi, Y. Senba, et al., Improvement in stability of SPring-8 X-ray monochromators with cryogenic-cooled silicon crystals, J. Phys. Conf. Ser. 425 (2013) 052001.

[13] P. Kristiansen, J. Horbach, R. Doehrmann, et al., Vibration measurements of high-heat-load monochromators for DESY PETRA III extension, J. Synchrotron Radiat. 22 (2015) 879–885.

[14] C.Y. Xu, Optics and Engineering of Synchrotron Radiation, University of Science and Technology of China Press, Hefei, 2013, pp. 363–365, (in Chinese).